Progress In Electromagnetics Research M, Vol. 8, 195–205, 2009

DYADIC GREEN FUNCTIONS FOR COAXIAL TUBULAR FILTERS

R. Pazoki

Electromagnetic Laboratory
School of Electrical and Computer Engineering
Iran University of Science and Technology
Tehran, Iran

J. Rashed-Mohassel

Center of Excellence on Applied Electromagnetic Systems
School of Electrical and Computer Engineering
Faculty of Engineering
University of Tehran
Tehran, Iran

Abstract—In this work, the dyadic Green functions for different parts of a coaxial tubular filter are derived. Using the obtained data, it is possible to consider the circuit model of a coaxial tubular filter. Moreover, the reactance due to the discontinuity of the matching section (dielectric loaded part) is calculated.

1. INTRODUCTION

Tubular filter is a common kind of filter which belongs to the classification of lumped element filters. Usually, lumped-element filters are constructed using parallel-plate chip capacitors and air-wound inductors soldered into a small housing. Skilled manual labor is required to build and tune such a filter. Furthermore, it is often difficult to integrate them into an otherwise all-thin-film assembly [1]. To overcome these difficulties, popular realizations of lumped element filters are in microstrip or coaxial forms. A possible geometry of a tubular filter implemented with a coaxial transmission line is shown in Figure 1.

Corresponding author: R. Pazoki (raeza2@yahoo.com).

The coaxial tubular filter has an advantage of compact structure and wide relative bandwidth. The structure and its equivalent circuit are shown in Figure 1. As it can be seen in Figure 1, the structure can be divided into five parts; the dielectric loaded washer c_1, coaxial transmission line (C_d and L_d), the coupling capacitive C_2. In fact the coupling capacitive part is a coaxial cable with inner radius a and outer radius b as shown in Figure 1(b), the inductive and the capacitive parts (C_{cap} and L_{ind}). These parts are connected to each other through coupling apertures. The capacitance of this coupling aperture is $C_c = 2\pi\varepsilon d/\ln(\frac{b}{b-t})$ [2], where the parameters t and d are shown in Figure 1.

There are some analysis methods in literature concerning tubular filters [2–6], however, no effort has been made in order to full-wave analyze the coaxial structure. In the current work, the dyadic Green function of the three sections shown in Figure 1 has been found. This would be helpful in designing the capacitances and inductances of the structure. The dyadic Green function is a powerful means of analyzing electromagnetic problems, especially when the orientation of the source is not prescribed. Moreover, it is very suitable to be utilized in EM-softwares. In what follows dyadic Green function of different parts of a coaxial tubular filter is found.

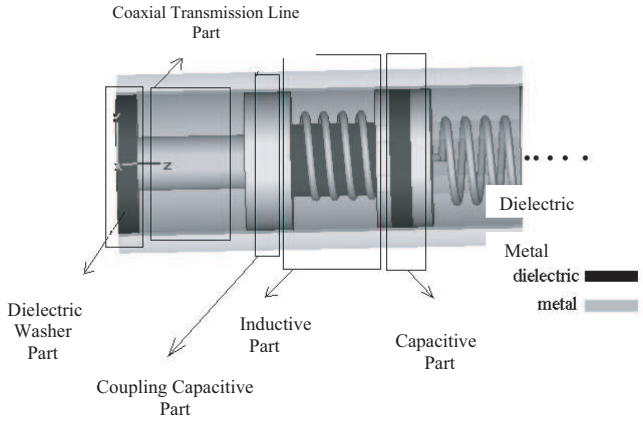

(a)

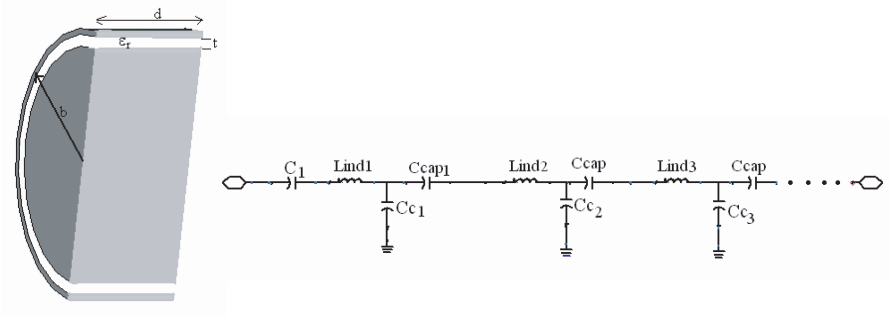

(b) (c)

Figure 1. (a) Geometry of a coaxial cable tubular filter, (b) extended view of the coupling capacitive part, and (c) the equivalent circuit of the structure.

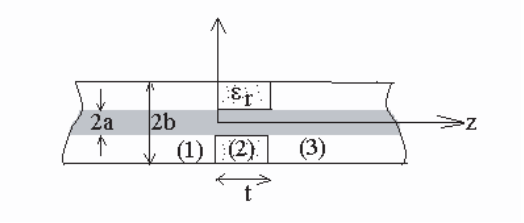

Figure 2. The dielectric loaded coaxial cable.

2. DYADIC GREEN FUNCTION OF THE DIELECTRIC-LOADED PART

Figure 2, shows the schematic of the dielectric loaded part, this part is usually used to match the filter to the input connector.

To derive the dyadic Green function of this configuration, the method of scattering superposition [7] is used as follows

$$\overline{\overline{G_e^{11}}}(\bar{R},\bar{R}') = \overline{\overline{G_{e1}}}(\bar{R},\bar{R}') + \overline{\overline{G_{es}^{11}}}(\bar{R},\bar{R}') \quad (1)$$

$$\overline{\overline{G_e^{12}}}(\bar{R},\bar{R}') = \overline{\overline{G_{es}^{12}}}(\bar{R},\bar{R}') \quad (2)$$

$$\overline{\overline{G_e^{13}}}(\bar{R},\bar{R}') = \overline{\overline{G_{es}^{13}}}(\bar{R},\bar{R}') \quad (3)$$

where $\overline{\overline{G_e^{ij}}}(\bar{R},\bar{R}')$ is the electric dyadic Green function in medium j due to the source in medium i. $\overline{\overline{G_{e1}}}(\bar{R},\bar{R}')$ is the electric dyadic Green function of the first kind i.e., $\overline{\overline{G_{e1}}}(\bar{R},\bar{R}') = 0$ on the boundary, and is

defined as follows [7]

$$\overline{\overline{G_{e1}}} = -\frac{1}{k^2}\hat{z}\hat{z}\delta(R-R') + C_{00}\underset{eoo}{\bar{N}}(\pm k)\,\bar{N}'_{eoo}(\mp k) + \sum_{n,\lambda}\bar{N}_{eon\lambda}(\pm k_\lambda)\bar{N}'_{eon\lambda}(\mp k_\lambda) + \sum_{n,\mu}\bar{M}_{eon\mu}(\pm k_\mu)\bar{M}'_{eon\lambda}(\mp k_\mu) \quad (4)$$

in which

$$C_{00} = 1/(4\pi^2 I0) \quad (5)$$

$$\bar{N}_{eoo}(\pm k) = \frac{1}{|k|}\nabla\times\nabla\times(\ln(r)e^{jkz}\hat{z}) \quad (6)$$

$$\bar{M}_{eon\lambda}(\pm k_\lambda) = \nabla\times\left[S_n(\lambda r)\ \begin{matrix}\cos\\ \sin\end{matrix}\ n\phi e^{j\pm k_\lambda z}\hat{z}\right] \quad (7)$$

$$\bar{N}_{eon\lambda}(\pm k_\lambda) = \frac{1}{\kappa_\lambda}\nabla\times\bar{M}_{eon\lambda}(\pm k_\lambda) \quad (8)$$

$$\bar{M}_{eon\mu}(\pm k_\mu) = \nabla\times\left[T_n(\mu r)\ \begin{matrix}\cos\\ \sin\end{matrix}\ n\phi e^{j\pm k_\mu z}\hat{z}\right] \quad (9)$$

$$\bar{N}_{eon\mu}(\pm k_\mu) = \frac{1}{\kappa_\mu}\nabla\times\bar{M}_{eon\mu}(\pm k_\mu) \quad (10)$$

where

$$\kappa_\lambda = (\lambda^2+h^2)^{1/2} \quad (11a)$$

$$\kappa_\mu = (\mu^2+h^2)^{1/2} \quad (11b)$$

$$S_n(\lambda r) = Y_n(\lambda a)J_n(\lambda r) - J_n(\lambda a)Y_n(\lambda r) \quad (12)$$

$$T_n(\mu r) = Y'_n(\mu a)J_n(\mu r) - J'_n(\mu a)Y_n(\mu r) \quad (13)$$

J_n and Y_n denote, respectively, Bessel function and Neumann function of integral order. The eigenvalues λ and μ are solutions of characteristic equations, i.e.,

$$S_n(\lambda b) = Y_n(\lambda a)J_n(\lambda b) - J_n(\lambda a)Y_n(\lambda b) = 0 \quad (14)$$

$$T'_n(\mu b) = Y'_n(\mu a)J'_n(\mu b) - J'_n(\mu a)Y'_n(\mu b) = 0 \quad (15)$$

where the primed functions denote the derivative of these functions with respect to their arguments μa or μb. A complete tabulation of these values is not yet available [7]. For $a = 4.72\,\text{mm}$ and $b = 12.67\,\text{mm}$, some of these eigenvalues can be obtained from $S_n(\lambda b)$ and $T'_n(\mu b)$ which are plotted in Figures 3(a) and 3(b).

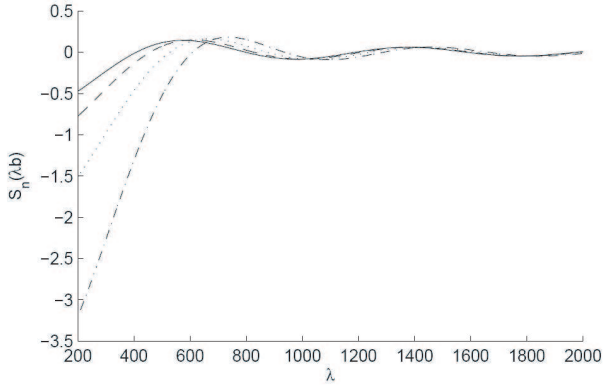

(a)

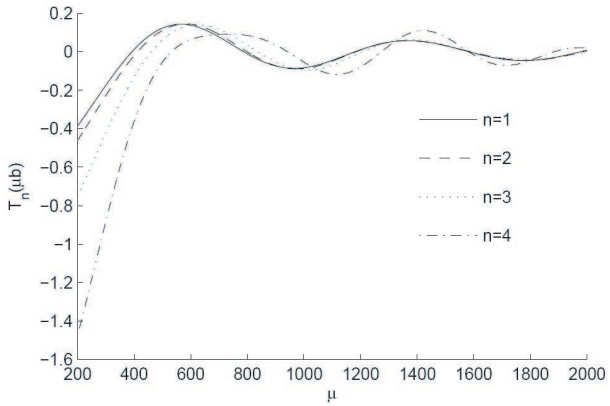

(b)

Figure 3. Eigenfunctions of coaxial cable with $a = 4.72\,\text{mm}$ and $b = 12.67\,\text{mm}$.

As it can be observed in Figure 3, the eigenvalues corresponding to different n's, are getting close as μ and λ increases.

$\overline{\overline{G}}_{es}^{ij}$ are assumed in following forms

$$\begin{aligned}\overline{\overline{G}}_{es}^{11} &= j\pi\Big[C_{00}\bar{N}_{eoo}(-k_1)\bar{N}'_{eoo}(-k_1)A_1 \\ &\quad + \sum_{n,\lambda}\frac{C_{n\lambda}}{k_{\lambda 1}}\bar{N}_{eon\lambda}(-k_{\lambda 1})\bar{N}'_{eon\lambda}(-k_{\lambda 1})A_2 \\ &\quad + \sum_{n,\mu}\frac{C_{n\mu}}{k_{\mu 1}}\bar{M}_{eon\mu}(-k_{\mu 1})\bar{M}'_{eon\lambda}(-k_{\mu 1})A_3\Big] \qquad (16a)\end{aligned}$$

$$\begin{aligned}\overline{\overline{G}}_{es}^{12} &= j\pi\Big[C_{00}\left\{B_1\bar{N}_{eoo}(-k_2)+B_2\bar{N}_{eoo}(-k_2)\right\}\bar{N}'_{eoo}(-k_1)\\ &+\sum_{n,\lambda}\frac{C_{n\lambda}}{k_{\lambda 1}}\left\{B_3\bar{N}_{eon\lambda}(k_{\lambda 2})+B_4\bar{N}_{eon\lambda}(-k_{\lambda 2})\right\}\bar{N}'_{eon\lambda}(-k_{\lambda 1})\\ &\sum_{n,\mu}\frac{C_{n\mu}}{k_{\mu 1}}\left\{B_5\bar{M}_{eon\mu}(k_{\mu 1})+B_6\bar{M}_{eon\mu}(-k_{\mu 1})\right\}\bar{M}'_{eon\lambda}(-k_{\mu 1})\Big] \quad (16b)\\ \overline{\overline{G}}_{es}^{13} &= j\pi\Big[C_{00}\bar{N}_{eoo}(k_1)\bar{N}'_{eoo}(-k_1)C_1\\ &+\sum_{n,\lambda}\frac{C_{n\lambda}}{k_{\lambda 1}}\bar{N}_{eon\lambda}(k_{\lambda 1})\bar{N}'_{eon\lambda}(-k_{\lambda 1})C_2\\ &\sum_{n,\mu}\frac{C_{n\mu}}{k_{\mu 1}}\bar{M}_{eon\mu}(k_{\mu 1})\bar{M}'_{eon\lambda}(-k_{\mu 1})C_3\Big] \quad (16c)\end{aligned}$$

and

$$\overline{\overline{G}}_{ms}^{ij} = \nabla\times\overline{\overline{G}}_{es}^{ij} \quad (17)$$

$$k_{\mu 1,2} = \left(k_{1,2}^2-\mu^2\right)^{1/2} \quad (18)$$

$$k_{\lambda 1,2} = \left(k_{1,2}^2-\lambda^2\right)^{1/2} \quad (19)$$

$$k_{1,2} = \omega\sqrt{\mu_0\varepsilon_{1,2}} \quad (20)$$

where A_i, B_i and C_i's are unknown coefficients to be determined. Using (1)–(16), subject to the boundary conditions

$$\hat{z}\times\left(\overline{\overline{G}}_e^{11}-\overline{\overline{G}}_{es}^{12}\right)\Big|_{z=0} = 0 \quad (21)$$

$$\hat{z}\times\nabla\times\left(\overline{\overline{G}}_e^{11}-\overline{\overline{G}}_{es}^{12}\right)\Big|_{z=0} = 0 \quad (22)$$

$$\hat{z}\times\left(\overline{\overline{G}}_e^{12}-\overline{\overline{G}}_{es}^{13}\right)\Big|_{z=t} = 0 \quad (23)$$

$$\hat{z}\times\nabla\times\left(\overline{\overline{G}}_e^{12}-\overline{\overline{G}}_{es}^{13}\right)\Big|_{z=t} = 0 \quad (24)$$

The calculated coefficients are
For TEM modes

$$B_1 = 2k_1(k_1-k_2)/\Delta \quad (25)$$

$$B_2 = 2k_1(k_1+k_2)/\Delta \quad (26)$$

$$A_1 = B_2-B_1+1 \quad (27)$$

$$C_1 = -\frac{k_2}{k_1}e^{j(k_2-k_1)t}B_1-\frac{k_2}{k_1}e^{-j(k_2+k_1)t}B_2 \quad (28)$$

where

$$\Delta = -(k_2 - k_1)^2 e^{-jk_2 t} + (k_2 + k_1)^2 e^{jk_2 t} \tag{29}$$

For TE modes

$$B_3 = 2k_1 k_{\lambda 1}(k_1 k_{\lambda 2} + k_2 k_{\lambda 1})/\Delta_1 \tag{30}$$

$$B_4 = 2k_1 k_{\lambda 1}(k_1 k_{\lambda 2} - k_2 k_{\lambda 1})/\Delta_1 \tag{31}$$

$$C_2 = \frac{k_{\lambda 2}}{k_{\lambda 1}}\left(e^{j(k_{\lambda 2} - k_{\lambda 1})t} B_3 - e^{-j(k_{\lambda 2} + k_{\lambda 1})t} B_4\right) \tag{32}$$

$$A_2 = 1 - \frac{k_{\lambda 2}}{k_{\lambda 1}}(B_4 - B_3) \tag{33}$$

$$\Delta_1 = 4k_1 k_2 k_{\lambda 1} k_{\lambda 2} \tag{34}$$

And for TM modes

$$B_5 = 2k_1 k_{\mu 1}(k_1 k_{\mu 1} + k_2 k_{\mu 2})/\Delta_2 \tag{35}$$

$$B_6 = 2k_1 k_{\mu 1}(k_2 k_{\mu 2} - k_1 k_{\mu 1})/\Delta_2 \tag{36}$$

$$C_3 = \frac{k_{\mu 2}}{k_{\mu 1}}\left(e^{j(k_{\mu 2} - k_{\mu 1})t} B_5 - e^{-j(k_{\mu 2} + k_{\mu 1})t} B_6\right) \tag{37}$$

$$A_3 = -1 + B_5 + B_6 \tag{38}$$

$$\Delta_2 = 4k_1 k_2 k_{\mu 1} k_{\mu 2} \tag{39}$$

Once the dyadic Green function of the structure is found, assuming a current excitation $\bar{J}_i(\bar{R})$ as

$$\bar{J}_i(\bar{R}) = \frac{\delta(z)\delta(\phi)}{(b-a)r}\hat{r} \tag{40}$$

$\overline{E}(\overline{R})$ is obtained from

$$\overline{E}(\overline{R}) = j\omega\mu_0 \iiint_V \overline{J}_i(\overline{R}) \cdot \overline{\overline{G}}_e(\overline{R}, \overline{R}')dR' \tag{41}$$

To obtain the impedance at $z = 0$, which its imaginary part is the reactance due to discontinuity of the waveguide, the complex power flow at $z = 0$ is used as follows

$$P = \iint_S \left(\bar{E}\left(\bar{R}\right) \times \bar{H}^*\left(\bar{R}\right)\right) \cdot \overline{ds} = Z|I|^2 = Z \tag{42}$$

In Equation (42), $\bar{J}_i$ is chosen such that $I = \iint_s \bar{J}_i \cdot \overline{ds} = 1$ and Z is readily obtained. As an example, assume a coaxial cable with

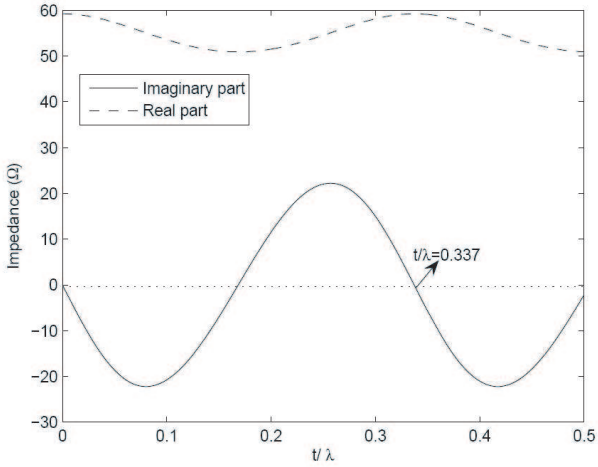

Figure 4. The impedance of the structure of Figure 2, at $z = 0$ for $a = 4.72\,\text{mm}$, $b = 12.67\,\text{mm}$ and $\varepsilon_r = 2.2$.

$a = 4.72\,\text{mm}$, $b = 12.67\,\text{mm}$ and $\varepsilon_r = 2.2$ (see Figure 2). For these values, the impedance at $z = 0$ is plotted in Figure 4.

It can be inferred from Figure 4 that for $t = 0$, the impedance at $z = 0$ is the same as the characteristic impedance of a coaxial cable with the given dimensions. Moreover, the structure of Figure 2 is given in [7] as coaxial-line beads. The optimum dielectric thickness which renders minimum reflection in an infinite coaxial cable is $t = \frac{\lambda}{2\sqrt{\varepsilon_r}}$ [7], which ε_r is the relative permittivity of the bead. For $\varepsilon_r = 2.2$, it can be seen that $(t/\lambda)_{opt} = \frac{1}{2\sqrt{2.2}} = 0.337$ which exactly matches the point of zero reactance in Figure 4 with a real part equal to the characteristic impedance of the coaxial line.

3. DYADIC GREEN FUNCTION OF THE CAPACITIVE PART

The capacitive part of the coaxial tubular filter shown in Figure 2 is indeed a cylindrical cavity. The dyadic Green function of such a structure is available [8].

4. DYADIC GREEN FUNCTION OF THE INDUCTIVE PART

The geometry of the inductive part is shown in Figure 5.

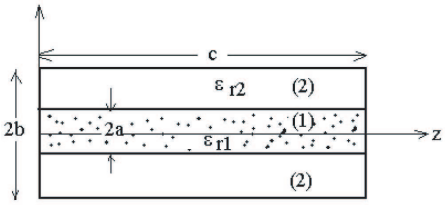

Figure 5. The inductive part of the coaxial tubular filter.

In this structure, both TE and TM modes are excited simultaneously. Following a similar procedure as in Section 3, we have

$$\bar{\bar{G}}_{es}^{12} = \sum_{n,\mu} \left[A_{1\,o}^{e}\, \bar{M}_{\lambda o2\,e}^{\,o}\begin{pmatrix} z \\ c-z \end{pmatrix} + B_{1\,o}^{e}\, \bar{N}_{\lambda o2\,o}^{\,e}\begin{pmatrix} z \\ c-z \end{pmatrix} \right] \bar{M}'_{\lambda o2\,e}^{\,o}\begin{pmatrix} c-z' \\ z' \end{pmatrix} + \left[A_{2\,o}^{e}\bar{M}_{\lambda o2\,o}^{\,e}\begin{pmatrix} z \\ c-z \end{pmatrix} + B_{2\,o}^{e}\bar{N}_{\lambda o2\,e}^{\,o}\begin{pmatrix} z \\ c-z \end{pmatrix} \right] \bar{N}'_{\lambda e2\,e}^{\,o}\begin{pmatrix} c-z' \\ z' \end{pmatrix} \quad (43a)$$

$$\bar{M}_{\lambda o2\,e}^{\,o}\begin{pmatrix} z \\ c-z \end{pmatrix} = \nabla \times \left[S_{1n}(\lambda_2 r) \begin{matrix} \cos \\ \sin \end{matrix} n\phi \cos k_\lambda \; \begin{matrix} z \\ c-z \end{matrix} \right] \quad (43b)$$

$$\bar{N}_{\lambda e2\,e}^{\,o}\begin{pmatrix} z \\ c-z \end{pmatrix} = \frac{1}{k}\nabla \times \nabla \times \left[T_{1n}(\lambda_2 r) \begin{matrix} \cos \\ \sin \end{matrix} n\phi \cos k_\lambda \; \begin{matrix} z \\ c-z \end{matrix} \hat{z} \right] \quad (43c)$$

$$T_{1n}(\lambda_2 r) = Y_n'(\lambda_2 b) J_n(\lambda_2 r) - J_n'(\lambda_2 b) Y_n(\lambda_2 r) \quad (43d)$$

$$S_{1n}(\lambda_2 r) = Y_n(\lambda_2 b) J_n(\lambda_2 r) - J_n(\lambda_2 b) Y_n(\lambda_2 r) \quad (43e)$$

$$\bar{\bar{G}}_{eo}^{11} = \sum_{n,\mu} \left[\bar{M}_{e\,\lambda o2}^{\,o}\begin{pmatrix} z \\ c-z \end{pmatrix} + \bar{N}_{o\,\lambda o2}^{\,e}\begin{pmatrix} z \\ c-z \end{pmatrix} \right] \bar{M}'_{\lambda o2\,e}^{\,o}\begin{pmatrix} c-z' \\ z' \end{pmatrix} + \left[\bar{M}_{o\,\lambda o2}^{\,e}\begin{pmatrix} z \\ c-z \end{pmatrix} + \bar{N}_{o\,\lambda o2}^{\,e}\begin{pmatrix} z \\ c-z \end{pmatrix} \right] \bar{N}'_{o\,\lambda e2}^{\,e}\begin{pmatrix} c-z' \\ z' \end{pmatrix} \quad (44a)$$

$$\bar{M}_{e\,\lambda o2}^{\,o}\begin{pmatrix} z \\ c-z \end{pmatrix} = \nabla \times \left[J_n(\lambda_2 r) \begin{matrix} \cos \\ \sin \end{matrix} n\phi \cos k_\lambda \; \begin{matrix} z \\ c-z \end{matrix} \widehat{z} \right] \quad (44b)$$

$$\bar{N}_{\substack{o\\e}\lambda e2}\begin{pmatrix} z \\ c-z \end{pmatrix} = \frac{1}{k}\nabla\times\nabla\times\left[J_n(\lambda_2 r)\ \begin{matrix}\cos\\ \sin\end{matrix}\ n\phi\cos k_\lambda\ \begin{matrix} z \\ c-z\end{matrix}\ \hat{z}\right] \quad (44c)$$

$$\overline{\overline{G}}_{es}^{11} = \sum_{n,\mu}\left[A_{\substack{3\\4}}{}^{\substack{e\\o}}\bar{M}_{\substack{o\\e}\lambda o1}\begin{pmatrix} z \\ c-z\end{pmatrix} + B_{\substack{3\\4}}{}^{\substack{e\\o}}\bar{N}_{\substack{e\\o}\lambda o1}\begin{pmatrix} z \\ c-z\end{pmatrix}\right]\bar{M}'_{\lambda o2}{}_{\substack{o\\e}}\begin{pmatrix} c-z' \\ z'\end{pmatrix}$$
$$+\left[A_{\substack{3\\4}}{}^{\substack{e\\o}}\bar{M}_{\substack{e\\o}\lambda o1}\begin{pmatrix} z \\ c-z\end{pmatrix} + B_{\substack{3\\4}}{}^{\substack{e\\o}}\bar{N}_{\substack{o\\e}\lambda o1}\begin{pmatrix} z \\ c-z\end{pmatrix}\right]\bar{N}'_{\lambda e2}{}_{\substack{o\\e}}\begin{pmatrix} c-z' \\ z'\end{pmatrix} \quad (45)$$

It should be noted that the generating functions in (43)–(44) are chosen such that they satisfy the boundary conditions at $z = 0$, $z = c$ and $r = b$. The boundary condition at the interface, $r = a$, requires

$$\hat{r}\times\left(\overline{\overline{G}}_e^{11} - \overline{\overline{G}}_{es}^{12}\right)\Big|_{r=a} = 0 \quad (46)$$

and

$$\hat{r}\times\nabla\times\left(\overline{\overline{G}}_e^{11} - \overline{\overline{G}}_{es}^{12}\right)\Big|_{r=a} = 0 \quad (47)$$

These conditions enables us to determine the scattering coefficients $A_{i_o^e}$ and $B_{i_o^e}$. To determine the eigenvalues of the structure the roots of the following determinant should be found

$$\begin{vmatrix} \frac{\partial TT_n(\lambda_2 r)}{\partial r} & \mp jk_\lambda SSn(\lambda_2 r) & \frac{\partial J_n(\lambda_1 r)}{\partial r} & \pm jk_\lambda J_n(\lambda_1 r) \\ 0 & \lambda_2^2\frac{\partial TT_n(\lambda_2 r)}{\partial r} & 0 & \lambda_1^2 J_n(\lambda_1 r) \\ \mp jk_\lambda k_2 SSn(\lambda_2 r) & k_2\frac{\partial TT_n(\lambda_2 r)}{\partial r} & \pm jk_\lambda k_1 J_n(\lambda_1 r) & \frac{\partial J_n(\lambda_1 r)}{\partial r} \\ k_2\lambda_2^2 SSn(\lambda_2 r) & 0 & \lambda_1^2 J_n(\lambda_1 r) & 0 \end{vmatrix}_{r=a} = 0$$

This completes our derivation for various dyadic Green functions of the coaxial tubular filter.

5. CONCLUSION

In this paper, dyadic Green functions of coaxial tubular filters have been obtained. This filter is a popular form among lumped element filters. First, the reactance due to the discontinuity of input (dielectric

loaded) part of the filter was considered. This part is necessary in order to match the filter to the input connector. Then, the dyadic Green function of inductive and capacitive parts of the structure was found. The analysis available in previous works only considers the dominant mode of the structure; however, using dyadic Green functions, when higher order modes are included, it is obvious that more accurate results can be achieved.

ACKNOWLEDGMENT

The authors appreciate Mr. H. Nemati for sharing some experimental results concerning coaxial tubular filters.

REFERENCES

1. Hong, J.-S. and M. J. Lancaster, *Microstrip Filters for RF/Microwave Applications*, John Wiley & Sons, Inc., 2001.
2. Cheng, D. K., *Field and Wave Electromagnetics*, Addison Wesley, 1983.
3. DeCarlo, R. and C. Meirina, "Parameter identification and adaptive control of an ultrafiltration process in hemodialysis," *Proceedings of the 2000 American Control Conference*, Vol. 5, 2967–2971, 2000.
4. Meirina, C. and R. A. DeCarlo, "Initial results in the adaptive control of ultrafiltration in hemodialysis," *Proceedings of the 38th IEEE Conference on Decision and Control*, Vol. 5, 5129–5130, 1999.
5. Huang, Q., J.-F. Liang, D. Zhang, and G.-C. Liang, "Direct synthesis of tubular bandpass filters with frequency-dependent inductors," *IEEE MTT-S International Microwave Symposium Digest*, Vol. 1, 371–374, 1998.
6. Wu, B., T. Su, B. Li, and C. H. Liang, "Design of tubular filter based on curve-fitting method," *Journal of Electromagnetic Waves and Applications*, Vol. 20, No. 8, 1071–1080, 2007.
7. Johnson, R. C., *Antenna Engineering Handbook*, 3rd edition, McGraw Hill, 1993.
8. Tai, C.-T., *Dyadic Green Functions in Electromagnetic Theory*, 2nd edition, IEEE Press, 1993.